

ASTROMETRY WITH THE HUBBLE SPACE TELESCOPE: TRIGONOMETRIC PARALLAXES OF SELECTED HYADS

BARBARA E. McARTHUR², G. FRITZ BENEDICT², THOMAS E. HARRISON³, WILLIAM VAN ALTENA⁴

Draft version July 12, 2018

ABSTRACT

We present absolute parallaxes and proper motions for seven members of the Hyades open cluster, pre-selected to lie in the core of the cluster. Our data come from archival astrometric data from FGS 3, and newer data for 3 Hyads from FGS 1R, both white-light interferometers on the *Hubble Space Telescope (HST)*. We obtain member parallaxes from six individual Fine Guidance Sensor (FGS) fields and use the field containing van Altena 622 and van Altena 627 (= HIP 21138) as an example. Proper motions, spectral classifications and VJHK photometry of the stars comprising the astrometric reference frames provide spectrophotometric estimates of reference star absolute parallaxes. Introducing these into our model as observations with error, we determine absolute parallaxes for each Hyad. The parallax of vA 627 is significantly improved by including a perturbation orbit for this previously known spectroscopic binary, now an astrometric binary. Compared to our original (1997) determinations, a combination of new data, updated calibration, and improved analysis lowered the individual parallax errors by an average factor of 4.5. Comparing parallaxes of the four stars contained in the *Hipparcos* catalog, we obtain an average factor of 11 times improvement with the *HST*. With these new results, we also have better agreement with *Hipparcos* for the four stars in common. These new parallaxes provide an average distance for these seven members, $\langle D \rangle = 47.5$ pc, for the core a $\pm 1 - \sigma$ dispersion depth of 3.6 pc, and a minimum depth from individual components of 16.0 ± 0.9 pc. Absolute magnitudes for each member are compared to established main sequences, with excellent agreement. We obtain a weighted average distance modulus for the core of the Hyades of $m-M=3.376 \pm 0.01$, a value close to the previous *Hipparcos* values, $m-M=3.33 \pm 0.02$.

Subject headings: astrometry — interferometry — Hyades — stars: distances

1. INTRODUCTION

What is the value of another parallax for the Hyades open star cluster? Though van Leeuwen (2009), Perryman *et al.* (1998) and de Bruijne *et al.* (2001) have established a distance to the Hyades using *Hipparcos* data, there remains a nagging worry; the Pleiades. We (Soderblom *et al.* 2005), Johns-Krull & Anderson (2005), and others (Gatewood *et al.* 2000, Pan *et al.* 2004, Munari *et al.* 2004) have independently measured a parallax that consistently differs from *Hipparcos*, a difference that remains in the recent *Hipparcos* re-reduction (van Leeuwen 2007). Recently Platais *et al.* (2007) found a similar distance discrepancy for the young cluster IC 2391. For many of the objects done both by *HST* and *Hipparcos* the agreement is good (e.g. Benedict & McArthur 2005). However, the Hyad parallax values from van Altena *et al.* (1997) were not included in the Benedict & McArthur (2005) comparison, because it was an initial analysis that pre-dated the improved calibration and Bayesian techniques that we later developed. Given the importance of the Hyades as a rung in the distance scale ladder (e.g., An *et al.* 2007b), and the overall importance of *Hipparcos* parallaxes to modern astrophysics, it would be useful to revisit the field and obtain an independent parallax and distance mod-

ulus for the Hyades and confirm that, as asserted in Narayanan & Gould (1999b,a), *Hipparcos* got it right.

Our targets are seven confirmed members of the Hyades cluster, with van Altena numbers (van Altena 1966) vA 310, 383, 472, 548, 622, 627, and 645. They are distributed on the sky in a roughly circular pattern centered on the cluster center, a consequence of an effort to pick Hyads in the core of the cluster. As pointed out in Perryman *et al.* (1998) there were significant differences between the *Hipparcos* parallaxes and the individual *HST* FGS parallaxes from van Altena *et al.* (1997). For the three brightest stars of the four in common between the two sets of observations (HIP 20563/vA 310, HIP 20850/vA 472, HIP 21123/vA 627) the *Hipparcos* parallaxes (van Leeuwen 2007) are between 22–38% larger than the 1997 *HST* values.

We anticipated that our improved techniques would significantly improve the precision of each Hyad's parallax from the average 1 mas of van Altena *et al.* (1997). This would potentially translate to a distance precision better than ~ 0.4 pc and an absolute magnitude precision of about 0.02 mag for each Hyades member. In addition to establishing an average parallax for the cluster center, these seven individual parallaxes will aid studies of the cluster depth. Our more precise individual absolute magnitudes could better establish the intrinsic width of the main sequence in the Hyades, identify contaminating binary systems, and provide an independent distance modulus.

In the last eleven years we have substantially improved the process whereby *HST* FGS fringe tracking data are

² McDonald Observatory, University of Texas, Austin, TX 78712

³ Department of Astronomy, New Mexico State University, Las Cruces, New Mexico 88003

⁴ Department of Astronomy, Yale University, New Haven CT 06520

turned into parallaxes (Benedict & McArthur 2005). This approach has been applied successfully, resulting in parallax results in many papers (Benedict *et al.* 1999, 2000a, 2000b, 2002a, 2002b, 2003, 2006; Beuermann *et al.* 2003, 2004; Harrison *et al.* 1999, 2004; McArthur *et al.* 1999, 2001, 2010; Roelofs *et al.* 2007; Soderblom *et al.* 2005), including parallaxes used for a recent recalibration of the Leavitt Law, the Galactic Cepheid Period-Luminosity relation (Benedict *et al.* 2007). We report here on applying the improvements to these archival (and newer) FGS data. This effort has resulted in far more accurate and precise parallaxes for seven Hyads.

Our reduction and analysis of these data is basically the same as for our previous work on galactic Cepheids (Benedict *et al.* 2007). Our extensive investigation of the astrometric reference stars provides an independent estimation of the line of sight extinction as a function of distance for all reference stars, a significant contributor to the uncertainty in their distances. Using vA 622/627 as an example throughout, we present the results of spectrophotometry of the astrometric reference stars, information required to derive absolute parallaxes from relative measurements (Section 3); and derive an absolute parallax for each Hyad (Section 4). We discuss some astrophysical consequences of these new, more precise distances (primarily the estimation of an independent distance modulus, Section 5), and summarize our findings in Section 6.

Bradley *et al.* (1991) and Nelan (2007) provide an overview of the FGS instrument and Benedict *et al.* (1999), Benedict *et al.* (2002c), Harrison *et al.* (2004), Benedict *et al.* (2007b) describe the fringe tracking (POS) mode astrometric capabilities of an FGS, along with the data acquisition and reduction strategies used in the present study. We time-tag all data with a modified Julian Date, $mJD = JD - 2400000.5$.

2. OBSERVATIONS AND DATA REDUCTION

We obtained from the *HST* archive forty orbits of Guaranteed Time Observation Fine Guidance Sensor (FGS) fringe tracking data secured by the *HST* Astrometry Science team using FGS 3. These data contain FGS observations of a total of 7 science targets (confirmed members of the Hyades open cluster listed in Table 1) and 36 reference stars. These data were previously analyzed and resulted in parallaxes for these Hyads published in van Altena *et al.* (1997b). We have also secured additional, more recent observations with FGS 1r for three of the Hyads.

Using the vA 622, vA 627 field as an example, Figure 1 shows the distribution on the sky of the Hyads and their reference stars taken from the Digitized Sky Survey, via *Aladin*. For the vA 622/627 seven sets of astrometric data were acquired with FGS 3 and five sets with FGS 1r the aggregate spanning 16 years, for a total of 164 measurements of vA 622, 627 and reference stars. Each data set required approximately 33 minutes of spacecraft time. The data were reduced and calibrated as detailed in Benedict *et al.* (2002c), Benedict *et al.* (2002b), McArthur *et al.* (2001), and Benedict *et al.* (2007b). At each epoch we measured reference stars and the target multiple times to correct for intra-orbit drift of the type seen in the cross filter calibration data shown in figure 1 of Benedict *et al.* (2002c).

Table 2 lists the epochs of observation for all six of our fields. Ideally (*cf.* Benedict *et al.* 2007) we obtain observations at each of the two maximum parallax factors⁴ at two distinct spacecraft roll values imposed by the requirement that *HST* roll to provide thermal control of a camera in the radial bay and to keep its solar panels fully illuminated throughout the year. This roll constraint generally imposes alternate orientations at each time of maximum positive or negative parallax factor over a typical two year campaign. A few observations at intermediate or low parallax factors usually allows a clean separation of parallax and proper motion signatures. Unfortunately, we have intermediate observations for only three of our prime targets, vA 548, vA 622, and vA 627. For these three fields we were able to take advantage of science instrument command and data handling (SIC&DH) computer problems that took the only other then operational science instrument (WFPC2) offline in late 2008. This situation opened a floodgate of FGS proposals, temporarily rendering *HST* nearly an '*all astrometry, all the time*' mission. Consequently, we obtained additional epochs well-separated in time from the original. This permitted a significantly better determination of relative proper motion for these targets (and for the perturbation orbit of vA 627, Section 4.1.2). For the other Hyad fields two-gyro guiding⁵ constraints did not permit re-observation.

3. SPECTROPHOTOMETRIC ABSOLUTE PARALLAXES OF THE ASTROMETRIC REFERENCE STARS

Because the parallax determined for the Hyads will be measured with respect to reference frame stars which have their own parallaxes, we must either apply a statistically derived correction from relative to absolute parallax (van Altena, Lee & Hoffleit 1995, hereafter YPC95) or estimate the absolute parallaxes of the reference frame stars listed in Table 3. In principle, the colors, spectral type, and luminosity class of a star can be used to estimate the absolute magnitude, M_V , and V-band absorption, A_V . The absolute parallax is then simply,

$$\pi_{abs} = 10^{-(V - M_V + 5 - A_V)/5} \quad (1)$$

The luminosity class is generally more difficult to estimate than the spectral type (temperature class). However, the derived absolute magnitudes are critically dependent on the luminosity class. As a consequence we appeal to reduced proper motions in an attempt to confirm the luminosity classes (see below).

3.1. Broadband Photometry

Our band passes for reference star photometry include: BV (CCD photometry from a 1m telescope at New Mexico State University) and JHK (from 2MASS⁶). Table 3

⁴ Parallax factors are projections along RA and Dec of the Earth's orbit about the barycenter of the Solar System, normalized to unity.

⁵ *HST* has a full compliment of six rate gyros, two per axis, that provide coarse pointing control. By the time these observations were in progress, three of the gyros had failed. *HST* can point with only two. To "bank" a gyro in anticipation of a future failure, NASA decided to go to two gyro pointing as standard operating procedure.

⁶ The Two Micron All Sky Survey is a joint project of the University of Massachusetts and the Infrared Processing and Analysis Center/California Institute of Technology

lists the visible and infrared photometry for all reference stars used in this study.

3.2. Spectroscopy, Luminosity Class-sensitive Photometry, and Reduced Proper Motion

The spectra from which we estimated spectral type and luminosity class come from the New Mexico State University Apache Point Observatory⁷. The dispersion was 0.61 Å/pixel with wavelength coverage 4101 – 4905 Å, yielding $R \sim 3700$. Classifications used a combination of template matching and line ratios. The brightest targets had about 1500 counts above sky per pixel, or $S/N \sim 40$, while the faintest targets had about 400 counts per pixel ($S/N \sim 20$). The spectral types for the higher S/N stars are within ± 1 subclass. Classifications for the lower S/N stars are ± 2 subclasses. Table 3 also lists the spectral types and luminosity classes for our reference stars.

We employ the technique of reduced proper motions to provide a confirmation of the reference star estimated luminosity class listed in Table 3. We obtain preliminary proper motions (μ) from UCAC3 (Zacharias et al. 2010) and/or PPMXL (Roeser et al. 2010), and J, K photometry from 2MASS for a one-degree-square field centered on each Hyad. With final proper motions from our astrometric solution (Section 4.1) we plot Figure 2, which shows $H_K = K + 5 \log(\mu)$ versus $(J - K)$ color index for 10,000 stars. If all stars had the same transverse velocities, Figure 2 would be equivalent to an H-R diagram. The Hyads and reference stars are plotted as ID numbers from Table 3. Errors in H_K , calculated using our final proper motions, are now ~ 0.3 mag.

3.3. Interstellar Extinction

To determine interstellar extinction we first plot these stars on several color-color diagrams. A comparison of the relationships between spectral type and intrinsic color against those we measured provides an estimate of reddening. Figure 3 contains a J - K vs V - K color-color diagram and reddening vector for $A_V = 1.0$. Also plotted are mappings between spectral type and luminosity class V and III from Bessell & Brett (1988) and Cox (2000) (hereafter AQ2000). Figure 3, and similar plots for the other measured colors, along with the estimated spectral types, provides an indication of the reddening for each reference star.

Assuming an $R = 3.1$ galactic reddening law (Savage & Mathis 1979), we derive A_V values by comparing the measured colors (Table 3) with intrinsic B - V , J - K , and V - K colors from Bessell & Brett (1988) and AQ2000. Specifically we estimate A_V from three different ratios, each derived from the Savage & Mathis (1979) reddening law: $A_V/E(J-K) = 5.8$; $A_V/E(V-K) = 1.1$; and $A_V/E(B-V) = 3.1$. The resulting average reference star A_V are collected in Table 3.

3.4. Adopted Reference Frame Absolute Parallaxes

We derive absolute parallaxes for the reference stars with M_V values from AQ2000 and the $\langle A_V \rangle$ derived from the photometry. Our parallax values are listed in Table 3. We produce errors on the absolute parallaxes by combining contributions from uncertainties in M_V and A_V ,

⁷ The Apache Point Observatory 3.5 m telescope is owned and operated by the Astrophysical Research Consortium.

which we have combined and set to 0.5 magnitude for each reference star. Individually, no reference star parallax is better determined than $\frac{\sigma_\pi}{\pi} = 23\%$. The average absolute parallax for the vA 622, 627 reference frame is $\langle \pi_{abs} \rangle = 1.2$ mas. As a sanity check we compare this to the correction to absolute parallax discussed and presented in YPC95 (section 3.2, fig. 2). Entering YPC95, fig. 2, with the vA 622 galactic latitude, $l = -19^\circ$, and average magnitude for the reference frame, $\langle V_{ref} \rangle = 16.0$, we obtain a galactic model-dependent correction to absolute of 1.3 mas, in agreement.

4. ABSOLUTE PARALLAXES OF THE HYADS

Sections 4.1.1-4 detail our astrometric modeling of the vA 622, 627 field. Any differences in modeling for other Hyads are noted in Section 4.1.5, below.

4.1. The vA 622, 627 Astrometric Model

With the positions measured by FGS 3 and FGS 1r we determine the scale, rotation, and offset “plate constants” relative to an arbitrarily adopted constraint epoch (the so-called “master plate”) for each observation set (the data acquired at each epoch). The mJD of each observation set is listed in Table 2. The vA 622, 627 reference frame contains 6 stars. We employ a four parameter model for those observations. For the vA 622, 627 field all the reference stars have colors similar to the science target. Nonetheless, we also apply the corrections for lateral color discussed in Benedict et al. (1999).

As for all our previous astrometric analyses, we employ GaussFit (Jefferys et al. 1988) to minimize χ^2 . The solved equations of condition for vA 622, 627 are:

$$x' = x + lc_x(B - V) \quad (2)$$

$$y' = y + lc_y(B - V) \quad (3)$$

$$\xi = Ax' + By' + C - \mu_x \Delta t - P_\alpha \pi_x \quad (4)$$

$$\eta = -Bx' + Ay' + F - \mu_y \Delta t - P_\delta \pi_y \quad (5)$$

where x and y are the measured coordinates from *HST*; lc_x and lc_y are the lateral color corrections from Benedict et al. 1999; and $B - V$ are those colors for each star. A and B are scale and rotation plate constants, C and F are offsets; μ_x and μ_y are proper motions; Δt is the epoch difference from the mean epoch; P_α and P_δ are parallax factors; and π_x and π_y are the parallaxes in x and y , which are constrained to be equal. We obtain the parallax factors (projections along RA and Dec of the Earth’s orbit about the barycenter of the Solar System normalized to unity) from a JPL Earth orbit predictor (Standish 1990), upgraded to version DE405. Additionally, given the previous identification of vA 627 as a spectroscopic binary (Griffin et al. 1985), and the higher than typical residuals modeling with only the above equations, we add Keplerian perturbation orbit terms to the model (c.f. McArthur et al. 2010, Benedict et al. 2010).

4.1.1. Prior Knowledge and Modeling Constraints

In a quasi-Bayesian approach the reference star spectrophotometric absolute parallaxes (Table 3) and proper motion estimates for the reference stars from PPMXL (Roeser et al. 2010) along with the lateral color calibration and B - V color indices were input as observations with associated errors, not as hardwired quantities

known to infinite precision. Input proper motion values have typical errors of 4–6 mas y^{-1} for each coordinate. To assess these input parallaxes and proper motions, the reference frame is modeled without the target to evaluate the goodness of fit of the a priori assumptions. After the target is included in the modeling, each reference star is systematically removed one at a time to assess impact on the target parallax and proper motions. Using these techniques we can assess the inputs for the reference frame, identify double stars in the reference frame, and occasionally solve for an orbit for the reference stars that have companions. Typically, at least 50–100 models are run in our process to determine the parallax. We essentially model a 3D volume of the space that contains our science target and reference stars, all at differing distances.

4.1.2. vA 627 Perturbation Orbit

The Keplerian elements for the best-fit perturbation orbit for vA 627 are presented in Table 5. Astrometry from FGS 3 and FGS1r and radial velocities from Griffin et al. (1985) were modeled simultaneously, using the methods described in McArthur et al. (2010). The orbit and residuals are presented in Figure 4. Assuming a mass for the K2 V primary, $M_A = 0.74M_{\odot}$, yields a secondary mass $M_B = 0.42M_{\odot}$, consistent with an infrared detection of the secondary spectrum by Bender & Simon (2008). The secondary is evidently an M2 V star. The estimated magnitude difference between vA 627 A (K2 V) and vA 627 B (M2 V) is $\Delta m = 3.6$ magnitudes. The total effect of component B on the apparent magnitude of the vA 627 system would be ~ -0.04 magnitudes. Hence, the effect of the companion on the size of the actual perturbation orbit (the photocentric orbit, c.f. van de Kamp 1967, Section 11.3) is negligible.

4.1.3. Assessing Reference Frame Residuals

The Optical Field Angle Distortion calibration (McArthur et al. 2002) reduces as-built *HST* telescope and FGS distortions with amplitude $\sim 1''$ to below 2 mas over much of the FGS field of regard. From histograms of the target and reference star astrometric residuals (Figure 5) we conclude that we have obtained satisfactory correction in the region available at all *HST* rolls. The resulting reference frame ‘catalog’ in ξ and η standard coordinates (Table 4) was determined, and it has a weighted $\langle \sigma_{\xi} \rangle = 0.6$ and $\langle \sigma_{\eta} \rangle = 0.7$ mas. Relative proper motions along RA (x) and Dec (y) are also listed in Table 4. The proper motion vector is listed in Table 6, as are astrometric results for the other Hyads, including catalog statistics.

To determine if there might be unmodeled - but possibly correctable - systematic effects at the 1 mas level, we plotted the vA 622, 627 reference frame x and y residuals against a number of spacecraft, instrumental, and astronomical parameters. These included x,y position within the pickle-shaped FGS field of regard; radial distance from the center of the FGS field of regard; reference star V magnitude and B-V color; and epoch of observation. We saw no obvious trends, other than an expected increase in positional uncertainty with reference star magnitude.

4.1.4. The Absolute Parallaxes of vA 622 and vA 627

Because of the low ecliptic latitude, most of the parallax signature is along RA. We obtain for vA 622 a final absolute parallax $\pi_{abs} = 24.11 \pm 0.30$ mas. This disagrees by almost 3σ with the van Altena et al. (1997a) determination, $\pi_{abs} = 21.6 \pm 1.1$ mas. We have achieved a significant reduction in formal error. For vA 627 we obtain a final absolute parallax $\pi_{abs} = 21.74 \pm 0.25$ mas, a value that differs substantially from the van Altena et al. (1997a) determination, $\pi_{abs} = 16.5 \pm 0.9$ mas. Our new vA 627 result agrees with previous parallax measurements from *Hipparcos*, $\pi_{abs} = 23.4 \pm 1.7$ mas (Perryman et al. 1998) and $\pi_{abs} = 22.75 \pm 1.22$ mas (van Leeuwen 2007). We note that this object is another for which the *Hipparcos* re-reduction has improved agreement with *HST*. This is not always the case. See Barnes (2009) for a few counter examples involving galactic Cepheids. Parallaxes and relative proper motion results for all fields from *HST* and four fields from *Hipparcos* are collected in Table 6. Even though *HST* both proper motion determinations are relative, the proper motion vectors for vA 622, 627 agree with the absolute motions determined by *Hipparcos*.

4.1.5. Modeling Notes on the Other Hyads

For all targets the reference star average data, *HST* (and if available) *Hipparcos* parallaxes and proper motions are collected in Tables 6 and 7. In all cases π_x and π_y are constrained to be equal. Three plate models are usually considered with *HST* astrometry. All models have offset terms C and F. The differences are in the scale terms. The first model has an equal scale in x and y , which is the model used for the vA 622 and vA 627 field using equations 4 and 5. The second model has separate scale in x and y , adding two parameters (D and E) to the first model.

$$\xi = Ax' + By' + C - \mu_x \Delta t - P_{\alpha} \pi_x \quad (6)$$

$$\eta = Dx' + Ey' + F - \mu_y \Delta t - P_{\delta} \pi_y \quad (7)$$

The third model has equal scale in x and y as the first model does, but also includes the addition of two radial terms in each axis (G and H).

$$\xi = Ax' + By' + G(x^2 + y^2) + C - \mu_x \Delta t - P_{\alpha} \pi_x \quad (8)$$

$$\eta = -Bx' + Ay' + H(x^2 + y^2) + F - \mu_y \Delta t - P_{\delta} \pi_y \quad (9)$$

The number of reference stars and the distribution of those stars dictates the model that is used. All fields are tested with all three models and the χ^2 and DOF are compared for goodness of fit.

vA 310 - This field provided six reference stars and we obtained seven usable epochs. We use a six parameter model, where two terms (D and E) provide independent scale in y shown in Equations 6 and 7. The *HST* parallax, $\pi_{abs} = 20.13 \pm 0.17$ mas agrees within the *Hipparcos* errors for both the 1997 and 2007 *Hipparcos* results. Our new parallax is considerably larger than the previous *HST* value, $\pi_{abs} = 15.4 \pm 0.9$, with a significantly improved formal error.

vA 383 - This field provided eight useful reference stars, but we were only able to secure six useable epochs. The astrometric model for this field required the addition of radial terms (G and H), using the 6 parameter model

shown in Equations 8 and 9, The introduction of the radial terms reduced the number of degrees of freedom by 13%, but reduced the χ^2 by 62% from the 4 parameter model shown in Equations 4 and 5. Our vA 383 parallax is $\pi_{abs} = 21.53 \pm 0.20$ mas. The original 1997 *HST* value was $\pi_{abs} = 16.0 \pm 0.9$ mas.

vA 472 - This field provided four useful reference stars and seven useable epochs. One of the reference stars, ref-86, is the only giant in our fields, obvious in the reduced proper motion diagram (Figure 2). In addition to the visual inspection of the classification spectrum and the evidence from the reduced proper motion diagram, a model input that assumes a dwarf classification for ref-86 increases χ^2 by 9%. The astrometric model for this field is a hybrid using four parameters (Equations 4 and 5) for one observation set containing an unusable reference star observation, and six parameters (Equations 6 and 7) for the other observation sets. The resulting reference frame 'catalog' in ξ and η standard coordinates (Table 4) was determined with a weighted $\langle \sigma_\xi \rangle = 0.9$ and $\langle \sigma_\eta \rangle = 0.9$ mas. Our vA 472 parallax is $\pi_{abs} = 21.70 \pm 0.15$ mas. This agrees with both the 1997 and 2007 *Hipparcos* results. Our new parallax with a formal error ~ 10 times smaller disagrees (4σ) with the van Altena (1997) result.

vA 548 - Seven reference stars, twelve epochs, and six parameter radial term modeling (Equations 8 and 9) yielded a parallax, $\pi_{abs} = 20.69 \pm 0.17$ mas, one that differs substantially from the 1997 *HST* value, $\pi_{abs} = 16.8 \pm 0.3$ mas.

vA 645 - Five reference stars, six epochs, and six parameter radial modeling (Equations 8, 9) yield $\pi_{abs} = 17.46 \pm 0.21$ mas. The vA 645 parallax agrees with an average of the 1997 and 2007 *Hipparcos* values. Again, the new *HST* result is larger (1.5σ) than the 1997 *HST* parallax.

The parallaxes from the previous analysis of *HST* FGS data (van Altena et al. 1997a); our new analysis, including newer data (Section 4.1); the original *Hipparcos* results (Perryman et al. 1997); and the recent re-reduction of the *Hipparcos* data (van Leeuwen 2007, 2009) are collected in Table 8.

4.2. New Analysis Improvements

In Table 8 we see that our new analysis yields results that have lower error, are significantly different than our earlier results and in general are more in agreement with both *Hipparcos* results. Several factors have contributed to this improvement. We now have a longer baseline on three of our 7 Hyads, and we were able to fit a perturbation orbit to vA 627. Our OFAD is greatly improved, with a baseline of 18 years instead of the 3 years of OFAD data we had when the initial Hyades study was done. Since the early OFAD, which depended upon ground-based proper motions of M35, we have been able to solve for *HST*-based motions, and we have added additional distortion fitting to the original OFAD model. We now have superior information about the reference frame, with improved proper motion and spectrophotometric parallaxes, which we treat as observations with error in the modelling, yielding absolute rather than relative parallaxes. All these factors combined yield more accurate and precise results. The older modelling technique used the ground based catalog technique of sum-

ming the reference star information to 0, which is more appropriate for a larger reference frame, and making adjustments from a relative to absolute parallax. The combination of the initial OFAD calibration with the older modelling technique resulted in parallaxes that were consistently lower than the new values. The new results are calibrated and modelled consistently with the other *HST* parallax objects discussed in Section 4.3.

4.3. Assessing *HST* External Error Using *Hipparcos*

For the four Hyads in common with *Hipparcos*, we obtain an internal parallax precision a factor of eleven better than *Hipparcos*. We assess our external accuracy by comparing these and past *HST* parallaxes with others from *Hipparcos*, specifically the re-reduction of van Leeuwen (2007). A total of twenty-eight stars are listed in Table 9, and include exoplanet host stars (ϵ Eri, v And, HD 138311, GJ 876, 55 Cnc, HD 38529), binary stars (Wolf 1062 AB, Feige 24, HD 33636, Y Sgr), M dwarfs (Proxima Cen, Barnard's Star, Wolf 1062 AB), Cepheids (1 Car, ζ Gem, β Dor, W Sgr, X Sgr, Y Sgr, FF Aql, T Vul, δ Cep, RT Aur), and the four Hyads of this paper (vA 310, vA 472, vA 627, vA645). We plot *Hipparcos* parallaxes against *HST* values in Figure 6. For three of our earliest analyses, rather than utilize spectrophotometrically-derived reference star parallaxes, we applied a model-based correction to absolute parallax discussed in van Altena et al. (1995). These are plotted in lighter grey. The regression line is derived from a GaussFit model (Jefferys et al. 1988) that fairly assesses errors in both *HST* and *Hipparcos* parallaxes. We note no significant scale difference over a parallax range $2 < \pi_{abs} < 770$ mas.

There are few notable outliers in Figure 6 and Table 9, objects further than $1 - \sigma$ from perfect agreement. Most of these are (for *Hipparcos*) faint stars. Regarding the two bright Cepheid outliers, RT Aur and Y Sgr, using *Hipparcos* parallaxes to produce a Period-Luminosity relation would place RT Aur at least 2.4 mag above the relation (at least because its *Hipparcos* parallax is negative). Y Sgr would lie 1.2 mag below. In this case Cepheid astrophysics supports the accuracy of the *HST* parallaxes (Barnes 2009). Apparently small differences can have significant astrophysical consequences. An *Hipparcos* Pleiades parallax ($\pi_{abs} = 8.32 \pm 0.13$ mas, van Leeuwen 2009) was not included in the Figure 6 impartial regression. That value differs only by 0.89 mas from the 2005 *HST* value, yet the equivalent difference of 0.2 magnitude in distance modulus calls much of modern stellar astrophysics into question (Soderblom et al. 2005). The Figure 6 regression and errors would predict an *Hipparcos* parallax for the Pleiades $\pi_{abs} = 7.63 \pm 0.12$, a 5σ difference from the measured *Hipparcos* value.

5. HYADES DEPTH AND DISTANCE MODULUS

The high-precision absolute parallaxes in Table 8 (column *HST11*) provide us an independent estimate of the depth of the Hyades core. Assuming a Gaussian distribution of Hyads yields a $\pm 1 - \sigma$ core dispersion of 3.6 pc. Back to front, differencing the distances of vA 622 and vA 645 we find a minimum diameter 16.0 ± 0.9 parsecs. The average distance of this particular sample is $D = 47.5$ pc.

By computing absolute magnitudes for these seven Hyads we can produce a sparsely populated color - absolute magnitude diagram and estimate a distance modulus, $m-M$, for the entire cluster. With parallaxes in hand (Table 8), we use vA 627 as an example to illustrate the steps required to obtain absolute magnitudes for these Hyads.

5.1. Absolute Magnitudes and the Lutz-Kelker-Hanson Bias

When using a trigonometric parallax to estimate the absolute magnitude of a star, a correction should be made for the Lutz-Kelker bias (Lutz & Kelker 1973) as modified by Hanson (1979). See Benedict et al. (2007b), section 5, for a more detailed rationale for the application of this correction to single stars. Because of the galactic latitude and distance of the Hyades, and the scale height of the stellar population of which it is a member, we calculate Lutz-Kelker-Hanson (LKH) bias assuming a disk distribution. The LKH bias is proportional to $(\sigma_\pi/\pi)^2$. Presuming that any member of the Hyades belongs to the same class of object as δ Cep (young Main Sequence stars), we scale the LKH correction determined for δ Cep in Benedict et al. (2002b) and obtain for vA 622, LKH = -0.001 magnitude, the maximum correction for any of these Hyads. Thus, LKH bias is a negligible component of the absolute magnitude error budget.

5.2. The Absolute Magnitude of vA 622

According to Taylor (2006) Hyades extinction is characterized by $E(B-V) \leq 0.001$ mag, obviating the necessity for extinction-induced corrections to absolute magnitude or color. Adopting for vA 622 $V = 11.90 \pm 0.01$ (SIMBAD) and the absolute parallax, $\pi_{abs} = 24.11 \pm 0.30$ mas from Table 8, we determine a distance modulus, $m-M = 3.09 \pm 0.04$. To obtain a final absolute magnitude, we would normally correct for interstellar extinction. However, with $E(B-V) \leq 0.001$ mag, $V_0 = V = 11.90$. The distance modulus and V_0 provide for vA 622 an absolute magnitude $M_V = 8.82 \pm 0.03$. This and the absolute magnitudes for the six other Hyads are collected in Table 10. All absolute magnitude errors contain only the contribution from the parallax uncertainty.

Figure 7 presents an HR diagram constructed from our Hyad absolute magnitudes (Table 10). The figure also contains a Hyades main sequence constructed with V , $B-V$ photometry from Joner et al. (2006) transformed to M_V using the van Leeuwen (2009) distance modulus, and an M67 main sequence from Sandquist (2004). There are too few stars with *HST* parallaxes to claim any systematic offset from the average Hyades/M67 main sequence.

5.3. A Hyades Distance Modulus

Including all seven stars, we obtain a weighted average Hyades distance modulus, $m-M = 3.376 \pm 0.012$. We note that from *Hipparcos* parallaxes both Perryman et al. (1998) and van Leeuwen (2009) obtain an average distance modulus of $m-M = 3.33 \pm 0.02$ from their entire sample of Hyads. With our entire (small) sample we get a distance modulus that is very close to *Hipparcos* 1997 or 2007. Our distance modulus determinations are listed in Table 11, along with other recent distance moduli. We

note the agreement between our value, and the results from the studies of binaries yielding orbital parallaxes (Torres et al. 1997a,b,c).

Those interested in an even more detailed description of the distance and structure of the Hyades will anticipate the results from *Gaia* (Lindegren et al. 2008). Parallax and proper motion precision factors of $10 - 100 \times$ better than *HST* are expected by ~ 2018 .

6. SUMMARY

We have reanalyzed older FGS 3 data of six fields and supplemental newer FGS1r astrometric data of two fields in the Hyades, containing seven confirmed Hyads. We employ techniques (Harrison et al. 1999; Benedict et al. 2007b) devised since the original analysis (van Altena et al. 1997a). These new absolute parallaxes now provide:

1. an average distance for these seven members, $D = 47.5$ pc with individual parallax errors lower by an average factor of 4.5 compared to the original study (van Altena et al. 1997a) and a factor of 11 times better than *Hipparcos* for the four stars in common,
2. a $\pm 1 - \sigma$ dispersion depth of 3.6 pc, and a minimum diameter 16.0 ± 0.9 pc,
3. absolute magnitudes for each member, yielding a sparsely populated main sequence,
4. a weighted average distance modulus of $m-M = 3.376 \pm 0.01$, a value that agrees within the errors to results from the orbital parallaxes of Hyades binaries (Torres et al. 1997a,b,c), and is very close to both *Hipparcos* results (Perryman et al. 1998; van Leeuwen 2009) ,
5. an independent parallax and distance modulus for the Hyades confirming the assertion of Narayanan & Gould (1999b) that *Hipparcos* 'got it right'.

Support for this work was provided by NASA through grants NAG5-1603 and AR-11746 from the Space Telescope Science Institute, which is operated by AURA, Inc., under NASA contract NAS5-26555. These results are based partially on observations obtained with the Apache Point Observatory 3.5 m telescope, which is owned and operated by the Astrophysical Research Consortium. This publication makes use of data products from the Two Micron All Sky Survey, which is a joint project of the University of Massachusetts and the Infrared Processing and Analysis Center/California Institute of Technology, funded by NASA and the NSF. This research has made use of the SIMBAD database and *Aladin*, both developed at CDS, Strasbourg, France; the NASA/IPAC Extragalactic Database (NED) which is operated by JPL, California Institute of Technology, under contract with the NASA; and NASA's Astrophysics Data System Abstract Service.

REFERENCES

An D., Terndrup D.M., & Pinsonneault M.H., 2007. *ApJ*, 671, 1640

Barnes T.G., 2009. In J.A. Guzik & P.A. Bradley, eds., *Stellar Pulsation: Challenges for Theory and Observation*, vol. 1170, 3–12. AIP
URL <http://link.aip.org/link/?APC/1170/3/1>

Bean J.L., McArthur B.E., Benedict G.F., et al., 2007. *AJ*, 134, 749

Bender, C. F. and Simon, M., 2008. *ApJ*, 689, 416

Benedict G.F., McArthur B., Chappell D.W., et al., 1999. *AJ*, 118, 1086

Benedict G.F. & McArthur B.E., 2005. In D. W. Kurtz, ed., *IAU Colloq. 196: Transits of Venus: New Views of the Solar System and Galaxy*, 333–346

Benedict G.F., McArthur B.E., Bean J.L., et al., 2010. *AJ*, 139, 1844

Benedict G.F., McArthur B.E., Feast M.W., et al., 2007a. *AJ*, 133, 2908

Benedict G.F., McArthur B.E., Feast M.W., et al., 2007b. *AJ*, 133, 1810

Benedict G.F., McArthur B.E., Forveille T., et al., 2002a. *ApJ*, 581, L115

Benedict G.F., McArthur B.E., Franz O.G., et al., 2000a. *AJ*, 119, 2382

Benedict G.F., McArthur B.E., Franz O.G., et al., 2000b. *AJ*, 120, 1106

Benedict G.F., McArthur B.E., Franz O.G., et al., 2001. *AJ*, 121, 1607

Benedict G.F., McArthur B.E., Fredrick L.W., et al., 2002b. *AJ*, 124, 1695

Benedict G.F., McArthur B.E., Fredrick L.W., et al., 2002c. *AJ*, 123, 473

Benedict G.F., McArthur B.E., Fredrick L.W., et al., 2003. *AJ*, 126, 2549

Benedict G.F., McArthur B.E., Gatewood G., et al., 2006. *AJ*, 132, 2206

Bessell M.S. & Brett J.M., 1988. *PASP*, 100, 1134

Beuermann K., Harrison T.E., McArthur B.E., et al., 2003. *A&A*, 412, 821

Beuermann K., Harrison T.E., McArthur B.E., et al., 2004. *A&A*, 419, 291

Bradley A., Abramowicz-Reed L., Story D., et al., 1991. *PASP*, 103, 317

Cox A.N., 2000. *Allen's Astrophysical Quantities*. AIP Press

de Bruijne J.H.J., Hoogerwerf R., & de Zeeuw P.T., 2001. *A&A*, 367, 111

Gatewood G., Castelaz M., de Jonge J.K., et al., 1992. *ApJ*, 392, 710

Gatewood G., de Jonge J.K., & Han I., 2000. *ApJ*, 533, 938

Griffin R.F., Griffin R.E.M., Gunn J.E., et al., 1985. *AJ*, 90, 609

Gunn J.E., Griffin R.F., Griffin R.E.M., et al., 1988. *AJ*, 96, 198

Hanson R.B., 1979. *MNRAS*, 186, 875

Harrison T.E., Johnson J.J., McArthur B.E., et al., 2004. *AJ*, 127, 460

Harrison T.E., McNamara B.J., Szkody P., et al., 1999. *ApJ*, 515, L93

Jefferys W.H., Fitzpatrick M.J., & McArthur B.E., 1988. *Celestial Mechanics*, 41, 39

Johns-Krull C.M. & Anderson J., 2005. In F. Favata, G. A. J. Hussain, & B. Battick, ed., *13th Cambridge Workshop on Cool Stars, Stellar Systems and the Sun*, vol. 560 of *ESA Special Publication*, 683–+

Joner M.D., Taylor B.J., Laney C.D., et al., 2006. *AJ*, 132, 111

Lindgren L., Babusiaux C., Bailer-Jones C., et al., 2008. In W. J. Jin, I. Platais, & M. A. C. Perryman, ed., *IAU Symposium*, vol. 248 of *IAU Symposium*, 217–223

Lutz T.E. & Kelker D.H., 1973. *PASP*, 85, 573

Martioli E., McArthur B.E., Benedict G.F., et al., 2010. *ApJ*, 708, 625

McArthur B., Benedict G.F., Jefferys W.H., et al., 2002. In S. Arribas, A. Koekemoer, & B. Whitmore, eds., *The 2002 HST Calibration Workshop: Hubble after the Installation of the ACS and the NICMOS Cooling System*, 373–+

McArthur B.E., Benedict G.F., Barnes R., et al., 2010. *ApJ*, 715, 1203

McArthur B.E., Benedict G.F., Lee J., et al., 1999. *ApJ*, 520, L59

McArthur B.E., Benedict G.F., Lee J., et al., 2001. *ApJ*, 560, 907

McArthur B.E., Endl M., Cochran W.D., et al., 2004. *ApJ*, 614, L81

Morris S., 1992. *JRASC*, 86, 292

Munari U., Dallaporta S., Siviero A., et al., 2004. *A&A*, 418, L31

Narayanan V.K. & Gould A., 1999a. *ApJ*, 515, 256

Narayanan V.K. & Gould A., 1999b. *ApJ*, 523, 328

Nelan E.P., 2007. *Fine Guidance Sensor instrument Handbook*. STScI, Baltimore, MD, 16 ed.

Pan X., Shao M., & Kulkarni S.R., 2004. *Nature*, 427, 326

Perryman M.A.C., Brown A.G.A., Lebreton Y., et al., 1998. *A&A*, 331, 81

Perryman M.A.C., Lindegren L., Kovalevsky J., et al., 1997. *A&A*, 323, L49

Platais I., Melo C., Mermilliod J., et al., 2007. *A&A*, 461, 509

Roelofs G.H.A., Groot P.J., Benedict G.F., et al., 2007. *ApJ*, 666, 1174

Roeser S., Demleitner M., & Schilbach E., 2010. *AJ*, 139, 2440

Sandquist E.L., 2004. *MNRAS*, 347, 101

Savage B.D. & Mathis J.S., 1979. *ARA&A*, 17, 73

Soderblom D.R., Nelan E., Benedict G.F., et al., 2005. *AJ*, 129, 1616

Standish Jr. E.M., 1990. *A&A*, 233, 252

Taylor B.J., 2006. *AJ*, 132, 2453

Torres G., Stefanik R.P., & Latham D.W., 1997a. *ApJ*, 485, 167

Torres G., Stefanik R.P., & Latham D.W., 1997b. *ApJ*, 474, 256

Torres G., Stefanik R.P., & Latham D.W., 1997c. *ApJ*, 479, 268

Turner D.G., Garrison R.F., & Morris S.C., 1994. *JRASC*, 88, 303

van Altena W.F., 1966. *AJ*, 71, 482

van Altena W.F., Lee J.T., & Hoffleit E.D., 1995. *The General Catalogue of Trigonometric [Stellar] Parallaxes*. New Haven, CT: Yale University Observatory 4th ed. (YPC95)

van Altena W.F., Lee J.T., & Hoffleit E.D., 1997a. *Baltic Astronomy*, 6, 27

van Altena W.F., Lu C.L., Lee J.T., et al., 1997b. *ApJ*, 486, L123+

van de Kamp P., 1967. *Principles of Astrometry*. Freeman

van Leeuwen F., 2007. *Hipparcos, the New Reduction of the Raw Data*, vol. 350 of *Astrophysics and Space Science Library*. Springer

van Leeuwen F., 2009. *A&A*, 497, 209

Zacharias N., Finch C., Girard T., et al., 2010. *AJ*, 139, 2184

TABLE 1
 HYAD POSITIONS

vA	alias	RA (2000)	Dec
vA 310	HIP 20563	04 24 16.94	18 00 10.49
vA 383	Os 373	04 26 4.71	15 02 28.90
vA 472	HIP 20850	04 28 04.44	13 52 04.59
vA 548	BD +15°634	04 29 30.98	16 14 41.40
vA 622	HD 285849	04 31 31.96	17 44 59.10
vA 627	HIP 21123	04 31 37.10	17 42 35.20
vA 645	HIP 21138	04 31 52.47	15 29 58.14

TABLE 2
LOG OF OBSERVATIONS

Set	mJD	P_α^a	P_δ^b
vA 310			
1	49252.9445	0.96275	0.12569
2	49407.2201	-1.02765	-0.16291
3	49601.8487	1.03632	0.15393
4	49768.0651	-1.02281	-0.16692
5	49943.0840	1.00037	0.17376
6	50128.2371	-1.00929	-0.17027
7	50331.9210	1.03261	0.15368
vA 383			
2	49409.23137	-1.01368	-0.15877
3	49595.01153	1.028972	0.15971
4	49781.66987	-1.01164	-0.14403
5	49943.95244	0.98764	0.18495
6	50123.27825	-0.96919	-0.18435
7	50338.95611	0.99744	0.12854
vA 472			
1	49256.8956	0.92173	0.08047
2	49422.4591	-0.99017	-0.12253
3	49596.9344	1.02376	0.15284
4	49769.4250	-1.00417	-0.16806
5	49963.6348	1.02032	0.14884
6	50131.2614	-0.99739	-0.17496
7	50340.8985	0.98650	0.11606
vA 548			
1	49209.0390	0.97032	0.17966
2	49410.1872	-1.02079	-0.15306
3	49577.7603	0.98803	0.17667
4	49769.3545	-1.01492	-0.16245
5	49943.9986	0.99046	0.17542
6	50122.2276	-0.96516	-0.17525
7	50336.9947	1.01415	0.13361
8	54810.5938	-0.17239	-0.11979
9	54810.6340	-0.17302	-0.11993
10	54811.4594	-0.18770	-0.12178
11	54811.5662	-0.18950	-0.12206
12	54811.6592	-0.19123	-0.12223
vA 622, vA 627			
1	49227.0396	1.04440	0.15652
2	49408.2456	-1.02747	-0.15263
3	49582.1176	1.01468	0.16447
4	49758.3671	-0.97649	-0.16396
5	49943.8667	0.99558	0.16578
6	50159.1570	-0.99223	-0.12207
7	50331.9914	1.03557	0.14358
8	55082.2052	1.03586	0.14058
9	55086.7759	1.02332	0.13315
10	55087.0645	1.02224	0.13269
11	55087.5746	1.02047	0.13177
12	55089.5716	1.01252	0.12822
vA 645			
1	49410.30146	-1.01741	-0.15020
2	49582.04762	1.00243	0.17306
3	49770.49773	-1.01316	-0.15934
4	49944.06818	0.98478	0.17634
5	50159.96080	-0.97731	-0.10778
6	50339.02691	1.00585	0.12372

^a Parallax factor in Right Ascension

^b Parallax factor in Declination

TABLE 3
HYAD ASTROMETRIC REFERENCE STAR PHOTOMETRY, SPECTRAL
CLASSIFICATIONS, AND ESTIMATED SPECTROPHOTOMETRIC PARALLAXES

ID	V	B-V	V-K	J-K	SpT	M _V	A _V	π _{abs} (mas)
vA 310 ^a	10.01	1.02						
50	15.07	1.25	2.97	0.66	K1V	6.2	1.1	2.8±0.7
51	15.69	0.94	2.33	0.49	G1V	4.5	1.0	0.9±0.2
52	14.67	1.33	3.29	0.77	K1V	6.2	1.4	3.8±0.9
53	15.57	0.84	2.11	0.42	F4V	3.3	1.3	0.7±0.2
54	16.11	1.23	2.86	0.65	K1V	6.2	1.1	1.7±0.4
55	15.40	0.85	1.98	0.40	F4V	3.3	1.4	0.7±0.2
vA 383	12.2	1.45						
61	16.14	1.14	2.88	0.61	G2V	4.7	1.6	1.1±0.2
62	15.43	1.25	3.22	0.76	G7V	5.4	1.6	2.1±0.5
63	15.06	1.1	2.87	0.65	F5V	3.5	2.0	1.3±0.3
64	14.13	1.18	2.99	0.64	G3V	4.8	1.7	3.0±0.7
65	15.97	1.47	2.86	0.80	K1.5V	6.3	1.7	2.6±0.6
66	16.54	1.38	2.96	0.78	K1V	6.2	1.6	1.7±0.4
68	16.87	1.35	4.21	0.75	G7V	5.4	1.9	1.2±0.3
69	15.24	1.14	2.58	0.58	F3V	3.2	2.3	1.1±0.3
vA 472	9.1	0.8						
86	14.07	1.46	3.77	0.88	K1III	0.6	1.8	0.4±1.4
88	15.10	1.51	3.79	0.86	K3V	6.8	1.5	4.3±1.0
89	16.27	0.95	2.75	0.61	G0V	4.2	1.5	0.7±0.2
92	17.03	1.36	5.05	0.84	M2V	9.9	1.0	3.1±0.7
vA 548	10.32	1.16						
96	13.44	1.07	2.65	0.57	G2V	4.7	1.4	3.4±0.8
97	15.37	0.98	2.77	0.60	G0V	4.4	1.2	1.1±0.3
98	15.56	1.19	3.15	0.68	G1V	4.5	1.8	1.5±0.3
99	15.93	1.15	3.25	0.66	G2V	4.7	1.6	1.2±0.3
100	14.05	0.95	2.55	0.46	F3V	3.2	1.7	1.5±0.3
101	14.07	0.96	2.61	0.47	F4V	3.3	1.7	1.6±0.4
102	14.91	1.15	3.02	0.60	G3V	4.8	1.6	2.0±0.5
vA 622	11.9	1.41						
vA 627	9.53	0.99						
109	14.79	0.89	2.33	0.50	G0V	4.4	1.0	1.3±0.3
112	15.64	1	2.45	0.54	G2V	4.7	1.2	1.1±0.3
113	13.97	0.8	2.23	0.45	F4V	3.3	1.2	1.3±0.3
115	16.10	0.89	2.44	0.51	F4V	3.3	1.5	0.6±0.1
116	15.46	0.89	2.43	0.52	G1V	4.5	0.9	1.0±0.2
117	14.55	1	2.68	0.59	G5V	5.1	1.0	2.0±0.5
vA 645	11	1.21						
120	15.88	1.29	3.64	0.72	F7V	3.9	2.4	1.2±0.3
121	15.28	1.15	3.12	0.61	F4V	3.3	2.3	1.2±0.3
122	16.23	1.55	4.13	0.85	G2V	4.7	2.9	1.8±0.4
123	16.38	1.21	3.79	0.81	G5V	5.1	1.6	1.2±0.3
126	15.98	1.3	3.60	0.70	G1.5V	4.6	2.2	1.5±0.3

^a V, B-V for all but vA 645 from co-I Harrison (NMSU)

TABLE 4
vA 622, vA 627, AND REFERENCE STAR ASTROMETRIC DATA

ID	ξ ^a	η ^a	μ_x ^b	μ_y ^b	π_{abs} ^c
vA 622 ^d	-22.3540 \pm 0.0003	69.9153 \pm 0.0004	102.21 \pm 0.04	-32.60 \pm 0.03	24.11 \pm 0.30
vA 627	86.5143 \pm 0.0003	21.4862 \pm 0.0003	105.87 \pm 0.04	-30.86 \pm 0.04	21.74 \pm 0.25
113	-231.3496 \pm 0.0005	-40.4306 \pm 0.0005	0.53 \pm 0.06	-2.94 \pm 0.09	1.30 \pm 0.14
112	-283.1685 \pm 0.0006	-20.8358 \pm 0.0008	0.52 \pm 1.48	0.38 \pm 1.21	0.57 \pm 0.07
116	-300.6054 \pm 0.0011	-2.0963 \pm 0.0011	6.23 \pm 0.06	-5.77 \pm 0.07	1.11 \pm 0.12
109	-198.8201 \pm 0.0006	18.9788 \pm 0.0012	6.59 \pm 0.05	-8.81 \pm 0.05	1.29 \pm 0.14
111	234.1750 \pm 0.0024	-43.6231 \pm 0.0021	2.66 \pm 1.12	-2.54 \pm 1.14	0.56 \pm 0.06
115	276.3116 \pm 0.0015	35.7347 \pm 0.0019	3.08 \pm 0.62	-3.0 \pm 0.72	0.98 \pm 0.11
117	340.4222 \pm 0.0015	2.2211 \pm 0.0009	15.67 \pm 0.67	-16.64 \pm 0.55	1.96 \pm 0.24

^a ξ (RA) and η (Dec) are relative positions in arcseconds.

^b μ_x and μ_y are relative motions in mas yr⁻¹, where x and y are aligned with RA and Dec.

^c Absolute parallax in mas

^d RA = 4^h31^m31.96^s +17°44' 59"1, J2000, epoch = mJD 50331.9705

TABLE 5
ORBITAL ELEMENTS OF
PERTURBATION DUE TO vA 627
B

Parameter	Value
α_A	14.58 ± 0.24 mas
P	843.94 ± 0.34 d
P	2.31 ± 0.001 yr
T_0	48658 ± 4 mJD
e	0.20 ± 0.01
i	$134^\circ 1 \pm 0^\circ 9$
Ω	$251^\circ \pm 4^\circ$
ω	$334^\circ \pm 2^\circ$
K_1	6.34 ± 0.3 km s $^{-1}$
M_A	$0.83 \pm 0.05 M_\odot$
M_B	$0.42 \pm 0.05 M_\odot$

TABLE 6
REFERENCE FRAME STATISTICS AND HYAD PARALLAX AND PROPER MOTION

Parameter	vA
Hyad	310
<i>HST</i> Study Duration (y)	2.95
Observation Sets (#)	7
Ref stars (#)	6
Ref stars $\langle V \rangle$	15.42
Ref stars $\langle B-V \rangle$	1.07
$\langle \sigma_\xi \rangle$ (mas)	0.3
$\langle \sigma_\eta \rangle$ (mas)	0.4
<i>HST</i> π_{abs} (mas)	20.13 ± 0.17
<i>HST</i> Relative μ (mas y $^{-1}$)	114.44 ± 0.27
in Position Angle ($^\circ$)	106.1 ± 0.1
<i>HIP97</i> π_{abs} (mas)	19.39 ± 1.79
<i>HIP97</i> μ (mas y $^{-1}$)	117.51 ± 3.18
in Position Angle ($^\circ$)	106.4
<i>HIP07</i> π_{abs} (mas)	19.31 ± 1.93
<i>HIP07</i> μ (mas y $^{-1}$)	116.05 ± 3.52
in Position Angle ($^\circ$)	107.7

TABLE 7
REFERENCE FRAME STATISTICS AND HYAD PARALLAX AND PROPER MOTION

Parameter	vA
Hyad	548
<i>HST</i> Study Duration (y)	15.34
Observation Sets (#)	12
Ref stars (#)	7
Ref stars $\langle V \rangle$	14.74
Ref stars $\langle B-V \rangle$	1.09
$\langle \sigma_\xi \rangle$ (mas)	0.4
$\langle \sigma_\eta \rangle$ (mas)	0.3
<i>HST</i> π_{abs} (mas)	20.69 ± 0.17
<i>HST</i> Relative μ (mas y $^{-1}$)	105.74 ± 0.03
in Position Angle ($^\circ$)	101.18 ± 0.02
<i>HIP97</i> μ (mas y $^{-1}$)	110.25 ± 2.0
in Position Angle ($^\circ$)	106.3
<i>HIP07</i> π_{abs} (mas)	22.75 ± 1.22
<i>HIP07</i> μ (mas y $^{-1}$)	110.23 ± 1.36
in Position Angle ($^\circ$)	105.9

TABLE 8
HYAD ABSOLUTE PARALLAXES (MAS)

vA	HST(97) ^a	HST(11) ^b	HIP97 ^c	HIP07 ^d
310	15.40±0.9	20.13±0.17	19.35±1.79	19.31±1.93
383	16.00±0.9	21.53±0.20		
472	16.60±1.6	21.70±0.15	21.29±1.91	21.86±1.71
548	16.80±0.3	20.69±0.17		
622	21.60±1.1	24.11±0.30		
627	16.50±0.9	21.74±0.25	23.41±1.65	22.75±1.22
645	15.70±1.2	17.46±0.21	15.11±4.75	19.13±5.45
weighted average	16.80±0.24	20.81±0.19	21.19±1.00	21.72±0.87
average	16.94±0.99	21.05±0.21	19.79± 2.04	20.76±1.05
median	16.50±0.99	21.52±0.20	20.32± 2.04	20.59±1.05
<i>average_{HIP}</i> ^e	16.05±1.15	20.26±0.19	19.79±2.04	20.76±105
HIP mean parallax ^f			21.53±2.76±0.23	

^a Parallaxes from the original analysis (van Altena et al. 1997a)

^b Parallaxes from the present study (Section 4.1)

^c Parallaxes from the original *Hipparcos* reduction (Perryman et al. 1997)

^d Parallaxes from the *Hipparcos* re-reduction (van Leeuwen 2007)

^e Parallax average considering only those stars in common with *Hipparcos*

^f The mean parallax of selected *Hipparcos* stars (van Leeuwen 2009)

TABLE 9
HST PARALLAXES IN COMMON WITH *Hipparcos*

ID	π_{HST} ^a	$\pi_{Hipparcos}$ ^b	$\Delta_{Hipparcos}$ ^c	Δ_{HST} ^c
Proxima Cen ^{d,e}	769.7±0.3	771.64±2.6	3.17	-0.04
Barnard's Star ^{d,e}	545.5±0.3	548.31±1.51	3.49	-0.14
Feige 24 ^e	14.6±0.4	10.86±3.94	-3.97	0.04
Wolf 1062 AB ^{d,g}	98±0.4	97.85±2.95	-0.25	0.00
RR Lyr ^h	3.82±0.2	3.46±0.64	-0.60	0.06
delta Cep ⁱ	3.66±0.15	3.81±0.2	-0.09	0.05
HD 213307 ⁱ	3.65±0.15	3.69±0.46	-0.23	0.02
GJ 876 ^j	214.6±0.2	213.26±2.12	-1.19	0.01
55 Cnc ^k	79.78±0.3	80.55±0.7	0.53	-0.10
ϵ Eri ^l	311.37±0.11	310.95±0.16	-0.06	0.03
HD 33630 ^m	35.6±0.2	35.27±1.02	-0.54	0.02
HD 136118 ⁿ	19.35±0.17	21.48±0.55	1.70	-0.16
1 Car ^o	2.01±0.2	2.06±0.27	-0.16	0.09
ζ Gem ^o	2.78±0.18	2.71±0.17	-0.17	0.19
β Dor ^o	3.14±0.16	3.64±0.28	0.15	-0.05
W Sgr ^o	2.28±0.2	2.59±0.75	0.01	0.00
X Sgr ^o	3.00±0.18	3.39±0.21	0.05	-0.04
Y Sgr ^o	2.13±0.29	3.73±0.32	0.72	-0.59
FF Aql ^o	2.81±0.18	2.05±0.34	-0.83	0.23
T Vul ^o	1.9±0.23	2.31±0.29	0.07	-0.04
RT Aur ^o	2.4±0.19	-0.23±1.01	-2.83	0.10
HD38529 ^p	25.11±0.19	25.46±0.4	0.08	-0.02
v And ^q	73.71±0.10	74.25±0.72	0.37	-0.01
vA310 ^r	20.13±0.17	19.31±1.93	0.95	-0.01
vA472 ^r	21.70±0.15	21.86±1.71	3.07	-0.11
vA627 ^r	21.74±0.25	22.75±1.22	0.03	-0.01
vA645 ^r	17.46±0.21	19.13±5.45	3.45	-0.01

^a Parallaxes in mas from *HST*^b Parallaxes in mas from van Leeuwen (2007)^c Residuals in mas from the impartial regression, *Hipparcos* vs *HST* (Figure 6)^d Parallaxes resulting from analysis that used a Galaxy model-based correction to absolute parallax (YPC95)^e Parallax from Benedict et al. (1999)^f Parallax from Benedict et al. (2000a)^g Parallax from Benedict et al. (2001)^h Parallax from Benedict et al. (2002c)ⁱ Parallax from Benedict et al. (2002b)^j Parallax from Benedict et al. (2002a)^k Parallax from McArthur et al. (2004)^l Parallax from Benedict et al. (2006)^m Parallax from Bean et al. (2007)ⁿ Parallax from Martioli et al. (2010)^o Parallax from Benedict et al. (2007a)^p Parallax from Benedict et al. (2010)^q Parallax from McArthur et al. (2010)^r Parallax from this paper

TABLE 10
HYAD DISTANCE MODULI AND
ABSOLUTE MAGNITUDES

vA	V	m-M	M _v
310	10.01	3.43	6.53±0.018
383	12.20	3.35	8.86±0.023
472	9.03	3.32	5.71±0.015
548	10.33	3.39	6.91±0.018
622	11.90	3.09	8.81±0.027
627	9.55	3.31	6.24±0.025
645	11.00	3.79	7.21±0.026

TABLE 11
HYADES DISTANCE MODULI

m-M	Author	Method
3.28 ± 0.10	Gunn et al. (1988)	RV & Convergent Point
3.45	Morris (1992)	Convergent Point
3.16 ± 0.10	Gatewood et al. (1992)	Parallax of 51 Tauri
3.20 ± 0.06	Gatewood et al. (1992)	Mean parallaxes (1992)
3.2 ± 0.1	Turner et al. (1994)	Combined methods
3.40 ± 0.07	Torres et al. (1997b)	Orbital parallax, 51 Tau
3.38 ± 0.11	Torres et al. (1997c)	Orbital parallax, 70 Tau
3.39 ± 0.08	Torres et al. (1997a)	Orbital parallax, 78 Tau
3.42 ± 0.09	van Altena et al. (1997a)	<i>HST</i> FGS (older reduction and modeling)
3.86 ± 0.13	van Altena et al. (1997a)	<i>HST</i> FGS (unweighted average, all stars, Tables 8, 10)
3.32 ± 0.06	van Altena et al. (1997b)	Mean of ground-based parallaxes (YPC95)
3.33 ± 0.01	Perryman et al. (1998)	<i>Hipparcos</i>
3.33 ± 0.02	van Leeuwen (2009)	<i>Hipparcos</i> reanalysis
3.376 ± 0.01	this paper	<i>HST</i> FGS reanalysis

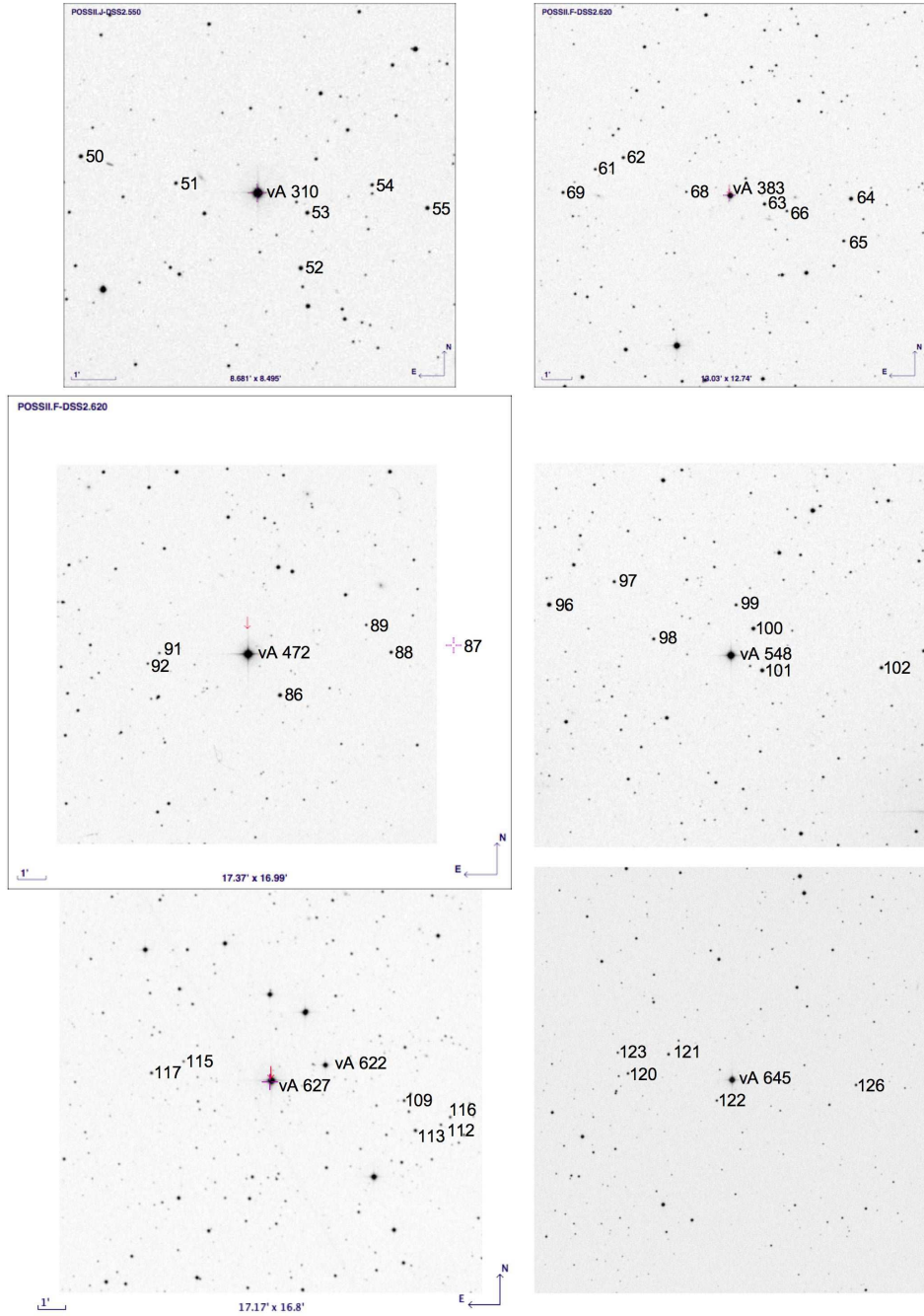


FIG. 1.— Finding charts for subject Hyads and astrometric reference stars. Labels are immediately to the right of each star. Where scales are not indicated, the box size is $13'1 \times 13'1$, north at top, east to left.

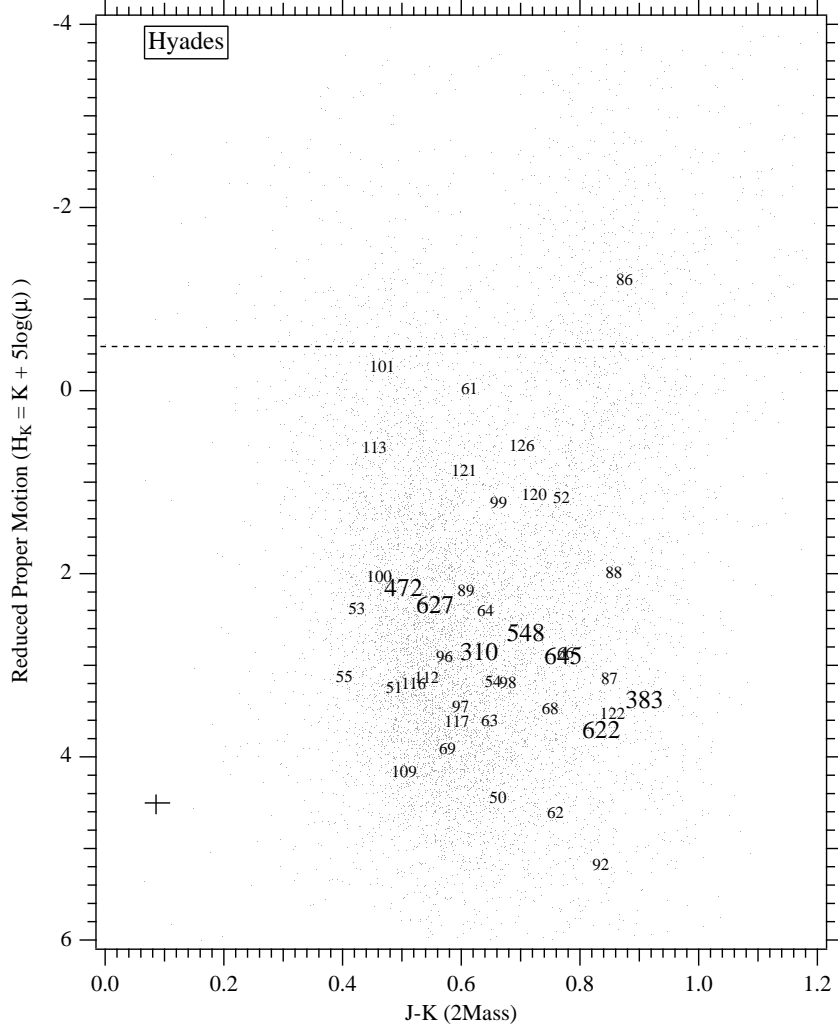


FIG. 2.— Reduced proper motion diagram for 10,000 stars in a 2° field centered on the Hyades. Star identifications are van Altena numbers and our internal ID for astrometric reference stars (Table 3). H_K for these stars is calculated using our final proper motions (Table 4). For a given spectral type giants and sub-giants have more negative H_K values and are redder than dwarfs in J-K. The horizontal line is an estimated demarcation between dwarfs (below) and giants (above) from a statistical analysis of the Tycho input catalog (D. Ciardi 2004, private communication). The cross in the lower left corner indicates representative errors along each axis.

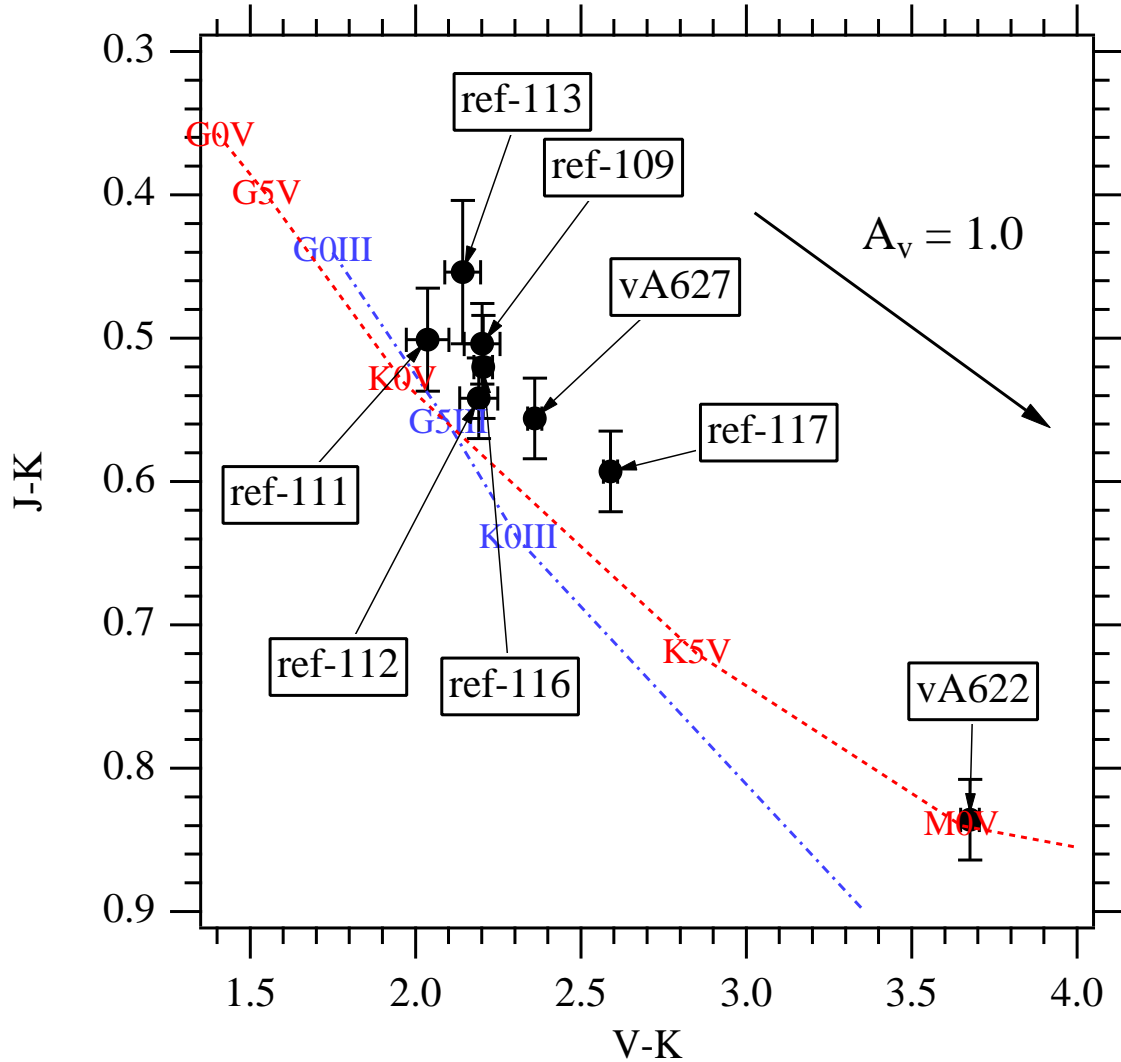


FIG. 3.— J-K vs V-K color-color diagram for the vA 622 vA 627 field. The dashed line is the locus of dwarf (luminosity class V) stars of various spectral types; the dot-dashed line is for giants (luminosity class III). The reddening vector indicates $A_V=1.0$ for the plotted color system.

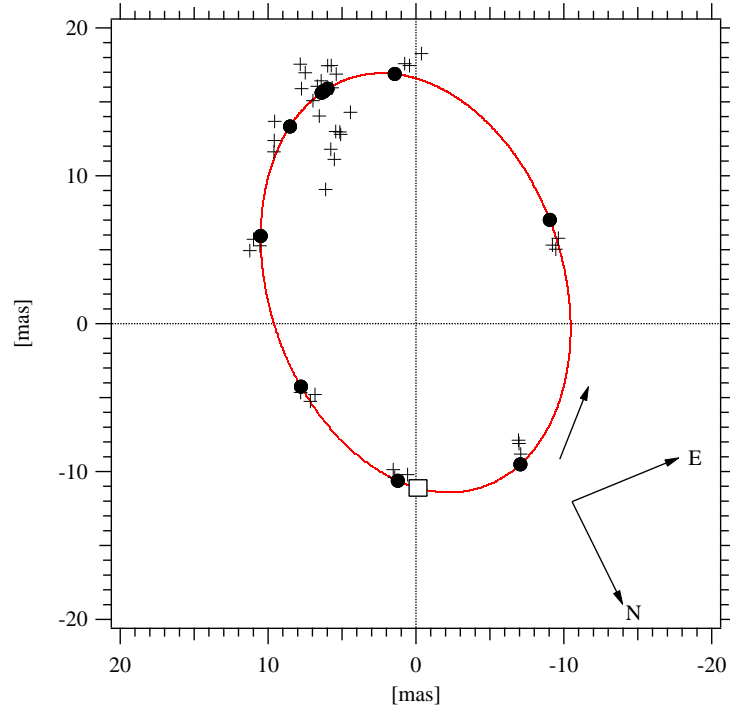


FIG. 4.— Final orbit and residuals for the vA 627 perturbation. The epoch of periastron passage is plotted as a square.

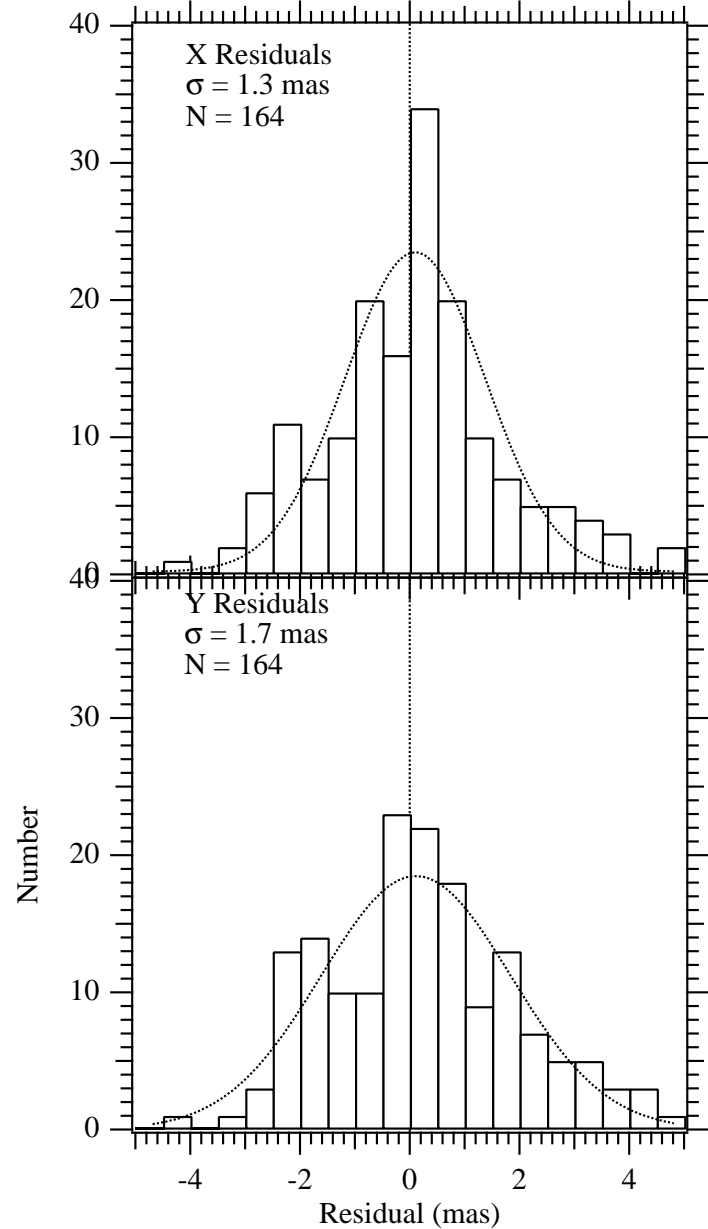


FIG. 5.— Histograms of x and y residuals obtained from modeling vA 622, vA 627, and the astrometric reference stars with Equations 4 and 5, including Keplerian orbit terms for vA 627. Distributions are fit with Gaussians whose σ 's are noted in the plots.

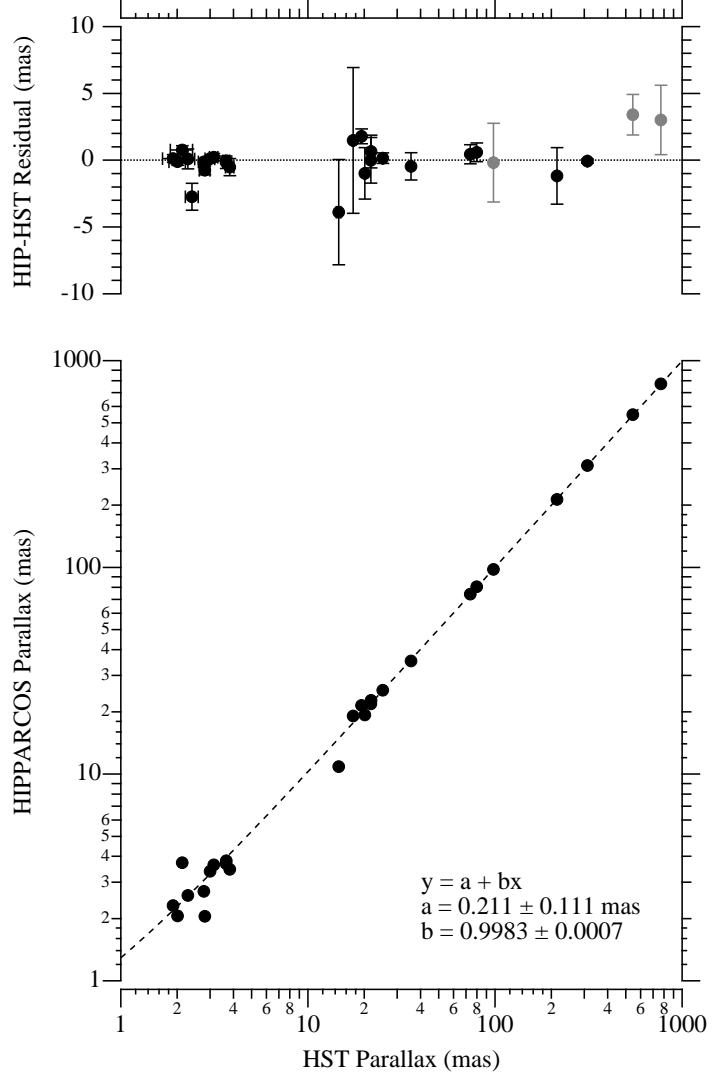


FIG. 6.— *Hipparcos* parallaxes from the re-reduction of van Leeuwen (2007) compared to all parallaxes from *HST* FGS (Table 9). The regression line is impartial, in that errors in both *Hipparcos* and *HST* parallaxes are considered (Jefferys et al. 1988). The few objects measured earlier (Proxima Cen, Barnard's Star, Wolf 1062 AB), employing a model-based correction to absolute parallax are plotted in lighter grey. Notable outliers include Feige 24 (faint CV), FF Aql, vA 645, and Y Sgr.

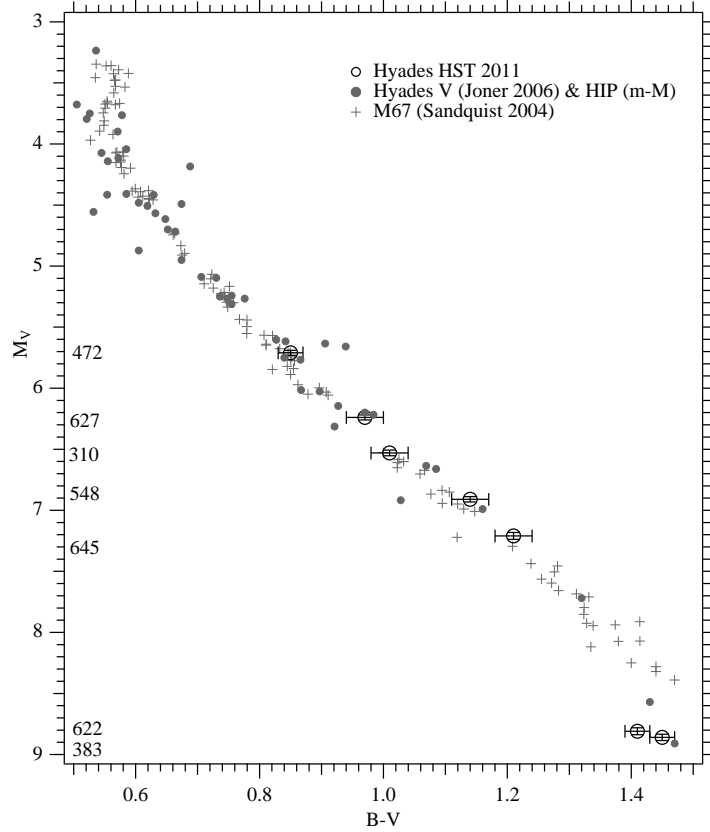


FIG. 7.— Absolute magnitude HR diagram for the seven Hyads with *HST* parallaxes. These are identified by van Altena number just interior to the left axis. Parallaxes used are from Table 8, ‘HST11’, the results from Section 4. Error bars are $\pm 1\sigma$. Also shown are M_V for the Hyads with photometry from Joner et al. (2006), assuming the van Leeuwen (2009) distance modulus, $m-M=3.33$. Also plotted are M67 M_V from Sandquist (2004). vA 627 is a known spectroscopic, now astrometric, binary. The *HST* parallaxes yield a weighted average distance modulus $m-M=3.376 \pm 0.01$.